

# Numerical study of the spherically-symmetric Gross-Pitaevskii equation in two space dimensions

Sadhan K. Adhikari

*Instituto de Física Teórica, Universidade Estadual Paulista, 01.405-900 São Paulo, São Paulo, Brazil*  
(October 23, 2018)

We present a numerical study of the time-dependent and time-independent Gross-Pitaevskii (GP) equation in two space dimensions, which describes the Bose-Einstein condensate of trapped bosons at ultralow temperature with both attractive and repulsive interatomic interactions. Both time-dependent and time-independent GP equations are used to study the stationary problems. In addition the time-dependent approach is used to study some evolution problems of the condensate. Specifically, we study the evolution problem where the trap energy is suddenly changed in a stable preformed condensate. In this case the system oscillates with increasing amplitude and does not remain limited between two stable configurations. Good convergence is obtained in all cases studied.

**PACS Number(s): 02.70.Rw, 02.60.Lj, 03.75.Fi**

## I. INTRODUCTION

Recent experiments [1] of Bose-Einstein condensation (BEC) in dilute bosonic atoms (alkali and hydrogen atoms) employing magnetic traps at ultra-low temperatures have intensified theoretical investigations on various aspects of the condensate [2–11]. The properties of the condensate are usually described by the nonlinear mean-field Gross-Pitaevskii (GP) equation [12], which properly incorporates the trap potential as well as the interaction among the atoms. The GP equation in both time-dependent and independent forms is formally similar to the Schrödinger equation with a nonlinear term. The effect of the interaction leads to the nonlinear term, which complicates the solution procedure. There have been several numerical studies of the GP equation in three space dimensions [3–7].

A Bose gas in lower dimensions – one and two dimensions – exhibits unusual features. For an ideal Bose gas BEC cannot occur in one and two space dimensions at a finite temperature because of thermal fluctuations [9,13]. The absence of BEC in one and two space dimensions has also been established for interacting uniform systems [13]. However, condensation can take place under the action of a trap potential [9,14] both for an ideal as well as interacting Bose gas.

Although, there has been no experimental realization of BEC in two space dimensions, this is a problem of great theoretical and experimental interests. In a usual experiment of BEC in three space dimensions under the action of a magnetic trap the typical thermal energy  $k_B T_c$  is assumed to be much larger than energy of oscillator quantum  $\hbar\omega$ , where  $k_B$  is the Boltzmann constant,  $T_c$  the critical temperature, and  $\omega$  the oscillator frequency. This will allow thermal oscillation in all three directions. Usually, in a typical experimental situation the oscillator frequencies in three different directions,  $x$ ,  $y$ , and  $z$ , are different. It is possible to obtain a quasi-two-dimensional BEC in a real three-dimensional trap by

choosing the frequency in the third direction  $\omega_z$  to satisfy  $\hbar\omega_z > k_B T_c > \hbar\omega_x, \hbar\omega_y$ . In that case the energy for thermal fluctuation is much smaller than the oscillator energy in the  $z$  direction. Consequently, any motion in the  $z$  direction will be frozen and this will lead to a realization of BEC in two space dimensions. The main features of BEC in two dimensions under the action of a harmonic trap has been discussed by Mullin recently [9]. Also, there has been consideration of BEC in low-dimensional systems for particles confined by gravitational field or by a rotational container [15]. Possible experimental configurations for BEC in spin-polarized hydrogen in two dimensions are currently being discussed [8,9].

Recent numerical studies of the GP equation in three space dimensions [2–7] in time-independent and time-dependent forms have emphasized that extensive care in numerical integration is needed to obtain good convergence. With the viability of experimental detection of BEC in two space dimensions [8], here we perform a numerical study of the time-dependent and time-independent GP equation in two space dimensions for an interacting Bose gas under the action of a harmonic oscillator trap potential. The interatomic interaction is taken to be both attractive and repulsive in nature.

The nonlinear time-dependent and time-independent GP equations can be compared with the corresponding two types of the linear Schrödinger equation. The stationary states in both cases have a trivial time dependence of the form  $\Psi(\mathbf{r}, t) = \exp(-iEt/\hbar)\Psi(\mathbf{r})$  where  $E$  is the parametric energy and  $t$  the time. As is well known the time-independent form of these equations determines the stationary function  $\Psi(\mathbf{r})$ , as in the hydrogen-atom problem. The time-dependent Schrödinger equation can also be directly solved to obtain the full time-dependent solution in the case of the stationary problems, from which the trivial time dependence  $\exp(-iEt/\hbar)$  can be separated. In fact, the time-dependent methods have been successfully used for the bound-state calculation in many areas of computational quantum chemistry [16]. This way of extracting the stationary solution from the

linear time-dependent Schrödinger equation continues as a powerful technique in the case of nonlinear time-dependent GP equations.

In this paper we solve the stationary BEC problem in two dimensions using both the time-dependent and time-independent GP equations in the cases of attractive and repulsive interatomic interactions and compare the two types of solutions. The time-independent GP equation is solved by integrating it with the Runge-Kutta rule complimented by the known boundary conditions at origin and infinity [17]. The time-dependent GP equation is solved by discretization and Gauss elimination method with the Crank-Nicholson-type rule complimented again by the known boundary conditions [17]. We find that both the time-dependent and time-independent approaches lead to good convergence for the stationary bound-state problem of the condensate. We also compare these solutions with the Thomas-Fermi approximation in the case of repulsive interatomic interaction.

In addition to obtaining the solution of the stationary problem the time-dependent GP equation can be used to study the intrinsic time-evolution problems with nontrivial time dependence and in this paper the time-dependent approach is also used to study some evolution problems. Specifically, we study the effect of suddenly altering the trapping energy on a preformed condensate. We find that in this case instead of executing sinusoidal oscillations between the stable initial and final configurations as in standard time-evolution problems governed by the linear Schrödinger equation, the condensate executes oscillations around the stable initial and final configurations with ever-growing amplitude.

In Sec. II we describe the time-dependent and time-independent forms of the GP equation. In Sec. III we describe the numerical method in some detail. In Sec. IV we report the numerical results and finally, in Sec. V we give a summary of our investigation.

## II. NONLINEAR GROSS-PITAEVSKII EQUATION

At zero temperature, the time-dependent Bose-Einstein condensate wave function  $\Psi(\mathbf{r}, \tau)$  at position  $\mathbf{r}$  and time  $\tau$  may be described by the self-consistent mean-field nonlinear GP equation [12]. In the presence of a magnetic trap this equation is written as

$$\left[ -\frac{\hbar^2}{2m}\nabla^2 + \frac{1}{2}m\omega^2 r^2 + gN|\Psi(\mathbf{r}, \tau)|^2 - i\hbar\frac{\partial}{\partial\tau} \right] \Psi(\mathbf{r}, \tau) = 0. \quad (2.1)$$

Here  $m$  is the mass of a single bosonic atom,  $N$  the number of atoms in the condensate,  $m\omega^2 r^2/2$  the attractive harmonic-oscillator trap potential,  $\omega$  the oscillator frequency, and  $g$  the strength of interatomic interaction. A

positive  $g$  corresponds to a repulsive interaction and a negative  $g$  to an attractive interaction. The normalization condition of the wave function is

$$\int_0^\infty d\mathbf{r} |\Psi(\mathbf{r}, t)|^2 = 1. \quad (2.2)$$

For a stationary solution the time dependence of the wave function is given by  $\Psi(\mathbf{r}, \tau) = \exp(-i\mu\tau/\hbar)\Psi(\mathbf{r})$  where  $\mu$  is the chemical potential of the condensate. If we use this form of the wave function in Eq. (2.1), we obtain the following stationary nonlinear time-independent GP equation [12]:

$$\left[ -\frac{\hbar^2}{2m}\nabla^2 + \frac{1}{2}m\omega^2 r^2 + gN|\Psi(\mathbf{r})|^2 - \mu \right] \Psi(\mathbf{r}) = 0. \quad (2.3)$$

The time-dependent equation (2.1) is equally useful for obtaining a stationary solution with trivial time dependence as well as for studying evolution processes with explicit time dependence.

Here we shall be interested in the spherically symmetric solution  $\Psi(\mathbf{r}, \tau) \equiv \varphi(r, \tau) = \varphi(r) \exp(-i\mu\tau/\hbar)$  to Eqs. (2.1) and (2.3), which can be written, respectively, as

$$\left[ -\frac{\hbar^2}{2m} \frac{1}{r} \frac{\partial}{\partial r} r \frac{\partial}{\partial r} + \frac{1}{2}m\omega^2 r^2 + gN|\varphi(r, t)|^2 - i\hbar\frac{\partial}{\partial\tau} \right] \varphi(r, \tau) = 0, \quad (2.4)$$

$$\left[ -\frac{\hbar^2}{2m} \frac{1}{r} \frac{d}{dr} r \frac{d}{dr} + \frac{1}{2}m\omega^2 r^2 + gN|\varphi(r)|^2 - \mu \right] \varphi(r) = 0. \quad (2.5)$$

The above limitation to the spherically symmetric solution (in zero angular momentum state) reduces the GP equations in two physical space dimensions to one-dimensional differential equations. We shall study numerically these one-dimensional equations in this paper.

As in Ref. [6], it is convenient to use dimensionless variables defined by  $x = r/a_{\text{ho}}$ , and  $t = \tau\omega/2$ , where  $a_{\text{ho}} \equiv \sqrt{\hbar/(m\omega)}$ ,  $\alpha = \mu/(\hbar\omega)$ ,  $\psi(x) = a_{\text{ho}}\sqrt{2mgN}\varphi(r)/\hbar$ , and  $\psi(x, t) = a_{\text{ho}}\sqrt{2\pi}\varphi(r, \tau)$ . In terms of these variables Eqs. (2.4) and (2.5) becomes, respectively,

$$\left[ -\frac{1}{x} \frac{\partial}{\partial x} x \frac{\partial}{\partial x} + x^2 + cn|\psi(x, t)|^2 - i\frac{\partial}{\partial t} \right] \psi(x, t) = 0, \quad (2.6)$$

$$\left[ -\frac{1}{x} \frac{d}{dx} x \frac{d}{dx} + x^2 + c|\psi(x)|^2 - 2\alpha \right] \psi(x) = 0. \quad (2.7)$$

where  $n \equiv mgN/(\pi\hbar^2)$  is the reduced number of particles and  $c = \pm 1$  carries the sign of  $g$ :  $c = 1$  corresponds to a repulsive interaction and  $c = -1$  corresponds to an

attractive interaction. The normalization condition (2.2) of the wave functions become

$$1 = \int_0^\infty |\psi(x, t)|^2 x dx = \frac{1}{n} \int_0^\infty |\psi(x)|^2 x dx. \quad (2.8)$$

We shall be using these two slightly different normalizations of the time-dependent and time-independent wave functions for future numerical convenience.

An interesting property of the condensate wave function is its mean-square radius defined by

$$\langle x^2 \rangle = \int_0^\infty x^2 |\psi(x, t)|^2 x dx = \frac{1}{n} \int_0^\infty x^2 |\psi(x)|^2 x dx. \quad (2.9)$$

### III. NUMERICAL METHOD

#### A. Boundary Condition

Both in time-dependent and time-independent approaches we need the boundary conditions of the wave function as  $x \rightarrow 0$  and  $\infty$ . For a confined condensate, for a sufficiently large  $x$ ,  $\psi(x)$  must vanish asymptotically. Hence the nonlinear term proportional to  $|\psi(x)|^3$  can eventually be neglected in the GP equation for large  $x$  and Eq. (2.7) becomes

$$\left[ -\frac{1}{x} \frac{d}{dx} x \frac{d}{dx} + x^2 - 2\alpha \right] \psi(x) = 0. \quad (3.1)$$

This is the equation for the oscillator in two space dimensions in the spherically symmetric state with solutions for  $\alpha = 1, 3, 5, \dots$  etc. A general classification of all the states of such an oscillator is well under control [18]. In the present BEC problem, Eq. (3.1) determines only the asymptotic behavior. If we consider Eq. (3.1) as a mathematical equation valid for all  $\alpha$  and large  $x$ , the asymptotic form of the physically acceptable solution is given by

$$\lim_{x \rightarrow \infty} \psi(x) = N_C \exp \left[ -\frac{x^2}{2} + (\alpha - 1) \ln x \right], \quad (3.2)$$

where  $N_C$  is a normalization constant. Equation (3.2) leads to the following asymptotic log-derivative

$$\lim_{x \rightarrow \infty} \frac{\psi'(x)}{\psi(x)} = \left[ -x + \frac{\alpha - 1}{x} \right], \quad (3.3)$$

which is independent of the constant  $N_C$  and where the prime denotes derivative with respect to  $x$ .

Next we consider Eq. (2.7) as  $x \rightarrow 0$ . The nonlinear term approaches a constant in this limit because of the regularity of the wave function at  $x = 0$ . Then one has the following usual conditions

$$\psi(0) = \text{constant}, \quad \psi'(0) = 0, \quad (3.4)$$

as in the case of the harmonic oscillator problem in two space dimensions [18]. Both the small- and large- $x$  behaviors of the wave function will be necessary for a numerical solution of the GP equation in time-dependent and time-independent forms.

#### B. Time-Dependent Approach: Evolution and Stationary Problems

First we describe the numerical method for solving the time-dependent equation (2.6). For a numerical solution it is convenient to make the substitution  $\psi(x, t) \equiv \phi(x, t)/x$  in this equation, when this equation becomes

$$\left[ -\frac{\partial^2}{\partial x^2} + \frac{1}{x} \frac{\partial}{\partial x} - \frac{1}{x^2} + x^2 + cn \frac{|\phi(x, t)|^2}{x^2} - i \frac{\partial}{\partial t} \right] \phi(x, t) = 0. \quad (3.5)$$

A convenient way to solve Eq. (3.5) numerically is to discretize it in both space and time and reduce it to a set of algebraic equations which could then be solved by using the known asymptotic boundary conditions. We discretize this equation by using a space step  $h$  and time step  $\Delta$  with a finite difference scheme using the unknown  $\phi_j^k$  which will be approximation of the exact solution  $\phi(x_j, t_k)$  where  $x_j = jh$  and  $t_k = k\Delta$ . As Eq. (3.5) involves both time and space variables it can be discretized in more than one way. The time derivative in Eq. (3.5) involves the wave function at times  $t_k$  and  $t_k + \Delta$ . As  $\Delta$  is small, the time-independent operations in this equation can be discretized by using the wave-function components at time  $t_k$  or  $t_{k+1} \equiv t_k + \Delta$ . If one uses the wave-function components at time  $t_k$ , Eq. (3.5) is discretized as

$$\begin{aligned} \frac{i(\phi_j^{k+1} - \phi_j^k)}{\Delta} &= -\frac{1}{h^2} [\phi_{j+1}^k - 2\phi_j^k + \phi_{j-1}^k] \\ &+ \frac{1}{2x_j h} [\phi_{j+1}^k - \phi_{j-1}^k] \\ &+ \left[ x_j^2 - \frac{1}{x_j^2} + cn \frac{|\phi_j^k|^2}{x_j^2} \right] \phi_j^k. \end{aligned} \quad (3.6)$$

This is an explicit differencing scheme, since, given  $\phi$  at  $t_k$  it is straightforward to solve for  $\phi$  at  $t_{k+1}$  [17]. One should start with an approximately known solution at  $t_k$  and propagate it in time until a converged solution is reached. We confirm in our study that this simple scheme leads to slow convergence and large unphysical oscillations in the solution.

One can express the derivatives on the right-hand-side of Eq. (3.6) in terms of the variables at time  $t_{k+1}$  [17]. Then the unknown  $\phi_j^{k+1}$  appears on both sides of the equation and one has an implicit scheme. We find that

the implicit scheme improves substantially the numerical accuracy and convergence rate. However, we find after some experimentation that if the right-hand-side of Eq. (3.6) is averaged over times  $t_k$  and  $t_{k+1}$  one has the best convergence. This is a semi-implicit scheme based on the Crank-Nicholson scheme for discretization [19]. We use the following rule to discretize the partial differential equation (3.5) [17,19]

$$\begin{aligned} \frac{i(\phi_j^{k+1} - \phi_j^k)}{\Delta} = & -\frac{1}{2h^2} \left[ (\phi_{j+1}^{k+1} - 2\phi_j^{k+1} + \phi_{j-1}^{k+1}) \right. \\ & \left. + (\phi_{j+1}^k - 2\phi_j^k + \phi_{j-1}^k) \right] \\ & + \frac{1}{4x_j h} [(\phi_{j+1}^{k+1} - \phi_{j-1}^{k+1}) + (\phi_{j+1}^k - \phi_{j-1}^k)] \\ & + \frac{1}{2} \left[ x_j^2 - \frac{1}{x_j^2} + cn \frac{|\phi_j^k|^2}{x_j^2} \right] (\phi_j^{k+1} + \phi_j^k). \end{aligned} \quad (3.7)$$

Similar discretization rule has been used for the solution of the GP equation in three space dimensions [3]. The first and second space derivatives of the wave function as well as the wave function itself have been approximated by the average over their values at the initial time  $t_k$  and the final time  $t_{k+1}$ . This procedure leads to accurate and stable numerical results. Considering that the wave function is known at time  $t_k$ , Eq. (3.7) is an equation in three unknowns –  $\phi_{j+1}^{k+1}$ ,  $\phi_j^{k+1}$  and  $\phi_{j-1}^{k+1}$ . In a lattice of  $N$  points Eq. (3.7) represents a tridiagonal set for  $j = 2, 3, \dots, (N-1)$ . This set has a unique solution if the wave functions at the two end points  $\phi_1^{k+1}$  and  $\phi_N^{k+1}$  are known. In the present problem these values at the end points are provided by the known asymptotic conditions. The tridiagonal set of equations is solved by the Gauss elimination method and back substitution [17] using a typical space step  $h = 0.0001$  and time step  $\Delta = 0.03$ . Although, the iterative method should work for any value of  $\Delta$ , we found the convergence to be faster with this value of  $\Delta$  and we used this value throughout the present investigation.

The time-dependent method could be used to study stationary as well as time-evolution problems. First we consider the stationary problem. For the ground and the first excited states of the condensate we start with the following analytically known wave functions of the harmonic oscillator problem (3.1) [18]:

$$\phi(x) = x\psi(x) = \sqrt{2x} \exp(-x^2/2), \quad (3.8)$$

$$\phi(x) = x\psi(x) = \sqrt{2x}(1-x^2) \exp(-x^2/2), \quad (3.9)$$

respectively, at an initial time  $t = 0$ . We then repeatedly propagate these solutions in time using the Crank-Nicholson-type algorithm (3.7). The boundary condition (3.4), that  $\phi(0) = 0$ , is implemented at each time step

[17]. Also, the solution at each time step will satisfy the asymptotic condition (3.2). Starting with  $cn = 0$ , at each time step we increase or decrease the nonlinear constant  $cn$  by an amount  $\Delta_1$  typically around 0.01. This procedure is continued until the desired final value of  $cn$  is reached. Then the final solution is iterated several times (between 10 to 40 times) to obtain a stable converged result. The resulting solution is the ground state of the condensate corresponding to the specific nonlinear constant  $cn$ . We found the convergence to be fast for small  $|cn|$ . However, the final convergence of the scheme breaks down if  $|cn|$  is too large. In practice these difficulties start for  $cn > 20$  for the ground state for a positive  $c$  (repulsive interaction) in a computational analysis in double precision. For an attractive interaction there is no such problem as the GP equation does not sustain a large nonlinearity  $|cn|$  as we comment in detail in the next section.

As the time dependence of these stationary states is trivial –  $\psi(x, t) = \psi(x) \exp(-i2\alpha t)$  – the chemical potential  $\alpha$  can be obtained from the propagation of the converged ground-state solution at two successive times, e.g.,  $\psi(x, t_k)$  and  $\psi(x, t_{k+1})$ . From the numerically obtained ratio  $\psi(x, t_k)/\psi(x, t_{k+1}) = \exp(i2\alpha\Delta)$   $\alpha$  can be obtained as the time step  $\Delta$  is known.

The time-dependent method could also be used to study evolution problems. One such evolution problem describes the fate of the condensate if the trap potential is removed or altered suddenly after the formation of the condensate. As a stable condensate is formed under the action of the trap potential, after a sudden change in the trap potential, the condensate will gradually modify with time. To study the time evolution of a condensate wave function as the trap is removed or altered suddenly, we have to start the time evolution of the known precalculated wave function of the condensate with the initial trap potential and allow it to evolve in time using the time-dependent GP equation with the full nonlinearity but with the altered trap potential, which could be zero.

### C. Time-Independent Approach

The time-independent GP equation (2.7) has the following structure

$$y' = G(x, \psi(y)), \quad (3.10)$$

with  $y = x\psi'$ , where the prime denotes the  $x$  derivative. With this realization, a numerical integration of Eq. (2.7) can be implemented using the following four-point Runge-Kutta rule [17,20] in steps of  $h$  from  $x_j$  to  $x_{j+1}$

$$\psi_{j+2} = \psi_{j+1} + h\psi'_{j+1}, \quad (3.11)$$

$$x_{j+1}\psi'_{j+1} = x_j\psi'_j + \frac{1}{6}(s_0 + 2s_1 + 2s_2 + s_3), \quad (3.12)$$

where

$$s_0 = hG(x_j, \psi_j), \quad (3.13)$$

$$s_1 = hG \left[ x_j + \frac{h}{2}, \psi_j + \frac{h(x_j \psi_j' + s_0/2)}{2(x_j + h/2)} \right], \quad (3.14)$$

$$s_2 = hG \left[ x_j + \frac{h}{2}, \psi_j + \frac{h(x_j \psi_j' + s_1/2)}{2(x_j + h/2)} \right], \quad (3.15)$$

$$s_3 = hG \left[ x_j + h, \psi_j + \frac{h(x_j \psi_j' + s_2)}{(x_j + h)} \right]. \quad (3.16)$$

Equation (2.7) is integrated numerically for a given  $\alpha$  using this algorithm starting at the origin ( $x = 0$ ) with the initial boundary condition (3.4) with a trial  $\psi(0)$  and a typical space step  $h = 0.0001$ . The integration is propagated to  $x = x_{\max}$ , where the asymptotic condition (3.3) is valid. The agreement between the numerically calculated log-derivative of the wave function and the theoretical result (3.3) was enforced to five significant figures. The maximum value of  $x$ , up to which we needed to integrate (2.7) numerically for obtaining this precision, is  $x_{\max} = 5$ . If for a trial  $\psi(0)$ , the agreement of the log-derivative can not be obtained, a new value of  $\psi(0)$  is to be chosen. The proper choice of  $\psi(0)$  was implemented by the secant method. Even with this method, sometimes it is difficult to obtain the proper value of  $\psi(0)$  for a given  $\alpha$ . Unless the initial guess is “right” and one is sufficiently near the desired solution, the method could fail, specially, for large  $|cn|$  and lead numerically to either the trivial solution  $\psi(x) = 0$  or an exponentially divergent nonnormalizable solution in the asymptotic region.

## IV. NUMERICAL RESULT

### A. Stationary Problem

First we consider the ground-state solution of Eq. (2.7) for different  $\alpha$  in cases of both attractive and repulsive interactions using the time-independent method. In the presence of the nonlinearity, for attractive (repulsive) interatomic interaction, the solutions of the GP equation for the ground state appear for values of chemical potential  $\alpha < 1$  ( $\alpha > 1$ ). The relevant parameters for the solutions – the wave-function at the origin  $\psi(0)$ , reduced number  $n$ , and mean-square radii  $\langle x^2 \rangle$  – are listed in Table I. The numerical integration was performed up to  $x_{\max} = 5$  with  $h = 0.0001$  where the asymptotic boundary condition (3.3) is implemented.

Using the known tabulated values of  $n$  in each case we also solved the time-dependent GP equation and the wave functions and energies so calculated agree well with the respective quantities calculated with the time-independent approach. The solutions were obtained using space step  $h = 0.0001$ , time step  $\Delta = 0.03$  and the parameter  $\Delta_1 \approx 0.01$ . The largest value of  $x$  used in discretization (3.7) is  $x_{\max} = 10$ . The wave functions for different values of  $\alpha$  (and  $n$ ) for the attractive and repulsive interparticle interactions for the cases shown in

Table I are exhibited in Figs. 1(a) and 1(b), respectively, where we plot  $\psi(x)$  versus  $x$  using the time-dependent and time-independent approaches. The curves in Figs. 1(a) and 1(b) appear in the same order as the rows in Table I and it is easy to identify the corresponding values of  $\alpha$  from the values of  $\psi(0)$  of each curve. From Figs. 1(a) and (b) we find that the nature of the wave function for these two cases are quite different. However, the wave functions calculated with time-dependent and time-independent approaches agree reasonably with each other.

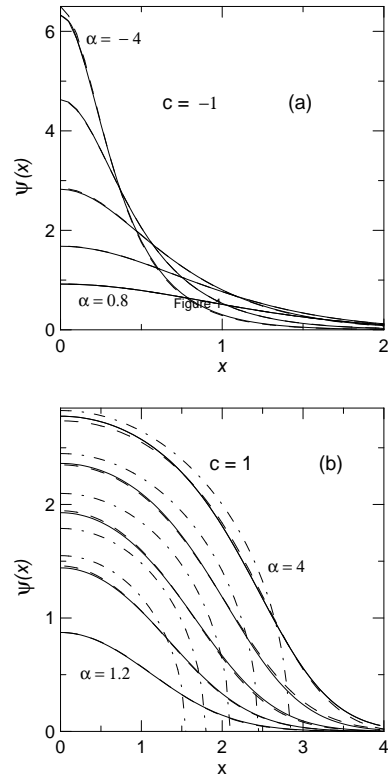


**Fig. 1.** Ground-state condensate wave function  $\psi(x)$  versus  $x$  for (a) attractive and (b) repulsive interparticle interactions using the time-dependent (dashed line) and time-independent (full line) approaches. The parameters for these cases are given in Table I. In the time-dependent method we used time step  $\Delta = 0.03$ ,  $\Delta_1 = 0.01$ , space step  $h = 0.0001$  and  $x_{\max} = 8$ , in the time-independent method we used space step  $h = 0.0001$  and  $x_{\max} = 5$ . In the case of the repulsive interparticle interaction we also show the solution (4.1) corresponding to the Thomas-Fermi approximation (dashed-dotted line). The curves appear in same order as in Table I. with the lowermost curve corresponding to the first row.

In the absence of previous solutions of this problem we compare the stationary solutions in the repulsive case ( $c = 1$ ) with those obtained via a well-known approximation, e.g., the Thomas-Fermi approximation. In this approximation the kinetic energy term in Eq. (2.7) is neglected and one has the following simple approximate solution

$$\psi(x) = \sqrt{2\alpha - x^2}, \quad (4.1)$$

for  $x^2 \leq 2\alpha$  and zero otherwise. In Fig. 1 (b) we also plot the Thomas-Fermi approximation (4.1). We find that as expected, for a large condensate, this approximation is a reasonable approximation. However, it turns out to be a bad approximation for a small condensate.

Table I: Parameters for the numerical solution of the GP equation (2.7) for  $c = \pm 1$  for the ground state wave function. The first four columns refer to the attractive interaction  $c = -1$  and the last four columns refer to the repulsive interaction  $c = 1$ .

$\alpha$	$\psi(0)$	$n$	$\langle x^2 \rangle$	$\alpha$	$\psi(0)$	$n$	$\langle x^2 \rangle$
1.0	0	0	0	1.0	0	0	0
0.8	0.9185	0.3663	0.9030	1.2	0.8719	0.4353	1.1027
0.4	1.6795	0.9147	0.7297	1.6	1.4415	1.5276	1.3219
-0.4	2.8255	1.4798	0.4757	2.2	1.9276	3.7509	1.6741
-2.0	4.6249	1.7695	0.2400	3.0	2.3626	7.8377	2.1679
-4.0	6.3252	1.8319	0.1385	4.0	2.7786	14.7609	2.8041

It is appropriate to comment on the numerical accuracy of the present time-dependent and independent methods, which seems to be limited typically by the difference between the time-dependent and independent solutions in Fig. 1. When the solution can be obtained numerically, as in the cases shown in Table I, the time-independent method can yield very accurate results. This accuracy can be increased by controlling the space step  $h$  and  $x_{\max}$ . This is not so in the case of the time-dependent method, where the numerical result exhibits small periodic oscillation after iteration specially for large values of  $|cn|$  which we detail below.

The numerical solution of the time-dependent method is independent of the space step  $h$  provided that a typical value around  $h = 0.0001$  is employed as in the present study. No visible difference in the solution is found if  $h$  is increased by a factor of 2 or 3. However, the solution is more sensitive to the number of time iterations, specially, for a large value of  $|cn|$ , for a fixed integration time step  $\Delta$  or the step  $\Delta_1$  by which the nonlinear constant in the GP equation is increased at each time step until the final value of  $cn$  is reached. We show this variation in Figs. 2 (a) and (b) where we plot  $|\psi(x, T)|$  as a function of reduced time  $T \equiv t/0.03$  for  $x = 0$  and 2 for different choices of  $\Delta$  and  $\Delta_1$  in the repulsive case for  $n = 3.7509$  and  $\alpha = 2.2$  corresponding to the fourth row of Table I. The zero of reduced time  $T$  is made to coincide with the time step  $t_k$  at which the full nonlinear constant  $cn$  is obtained for the first time during iteration. This choice of time will allow us to compare the fluctuations of the solution during the time propagation of the full GP equation. In Fig. 2(a) we present our results for  $\Delta = 0.03$  and for  $\Delta_1 = 0.018754$  and  $0.0046886$ . In Fig. 2(b) we present our results for  $\Delta_1 = 0.0046886$  and for  $\Delta = 0.03$ , and  $0.05$ . From Figs. 2 (a) and (b) we find that there is numerical oscillation of the solution with time in this approach which is independent of small variations of  $\Delta$  near

$0.03$  and  $\Delta_1$  around  $0.01$ . These oscillations determine the numerical error of the time-dependent approach and become larger when we employ a  $\Delta$  very different from  $0.03$ , or  $\Delta_1$  very different from  $0.01$ . The oscillations can really be large if an improper value of step  $\Delta$  or  $\Delta_1$  is chosen as can be seen from Fig. 2(b) for  $\Delta = 0.05$ . The results remain stable if we reduce these steps up to  $\Delta \sim 0.01$  and  $\Delta_1 \sim 0.003$ . For very small  $\Delta_1$  and  $\Delta$  accumulative errors also increase. This accumulative numerical error increases as the number of iterations is very large (several thousands) and a large number of iterations is needed to cover a given time interval with a small time step  $\Delta$ .

Table II: Amplitude of oscillation  $A(x, T)$  (in units of  $0.01$ ) of  $|\psi(x, T)|$  at different times  $T$  for  $x = 0$  and 2 calculated with  $\Delta = 0.03$  and  $\Delta_1 = 0.0046886$  in the repulsive case for  $cn = 3.7509$ . The average value of converged  $|\psi(0, T)| = 1.9310$  and  $|\psi(2, T)| = 0.6667$ .

$T =$	0	167	294	406	533	645	791
$ A(0, T) $	1.54	1.27	3.32	2.93	4.13	4.49	7.35
$T =$	0	162	291	400	536	637	789
$ A(2, T) $	0.77	0.95	1.13	1.33	1.43	2.01	2.77

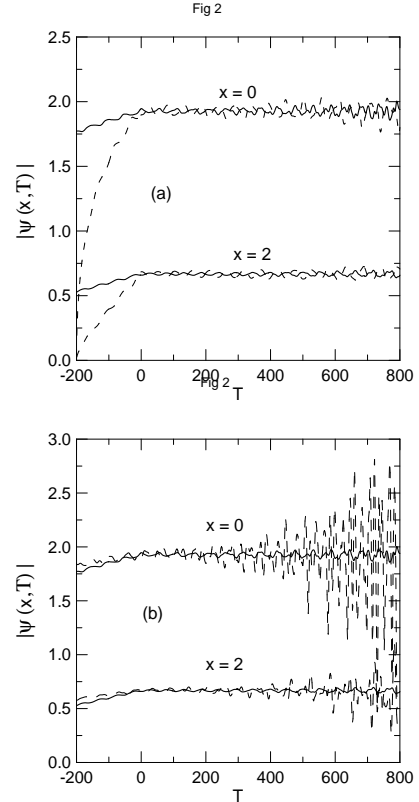


**Fig. 2.** Ground-state condensate wave function  $|\psi(x, T)|$  versus reduced time  $T \equiv t/0.03$  for  $x = 0$  and 2 in the repulsive case for the nonlinear constant  $cn = 3.7509$  for (a)  $\Delta = 0.03$ , and  $\Delta_1 = 0.0046886$  (full line), and  $0.018754$  (dashed line) and (b)  $\Delta_1 = 0.0046886$  and for  $\Delta = 0.03$  (full line), and  $0.05$  (dashed line). The zero of  $T$  is taken to be the time at which the full nonlinearity is achieved for the first time.

We show a quantitative account of the above oscillation in Table II where we plot the maximum error in  $|\psi(x, T)|$  (amplitude of oscillation of  $|\psi(x, T)|$ ) for  $x = 0$  and 2 at different times calculated with steps  $\Delta = 0.03$  and  $\Delta_1 = 0.0046886$ . We find that the error increases slowly, but not necessarily monotonically, with time. The average value of the converged  $|\psi(0, T)|$  is 1.9310 and that for  $|\psi(2, T)|$  is 0.6667. The maximum deviations from these values as shown in Table II do not occur at the same values of  $T$ . We find from Table II that for small  $T$  ( $\sim 0$ ) the maximum average error in  $|\psi(x, T)|$  is about 1%. For  $T \sim 800$  this maximum average error could be as high as 4%. As these errors are oscillating with time, at a given  $T$  this error could be smaller or even zero. Considering that we are dealing with nonlinear equations these errors are well within the acceptable limits. The errors shown in Table II would also be the typical errors in time-evolution problems which we study in the next subsection.

For repulsive interaction, it was increasingly difficult to find the solution of the GP equation using both time-dependent and time-independent methods for larger nonlinearity than those reported in Figs. 1 (a) and (b). The inputs of the time-independent method are  $\alpha$  and an appropriate  $\psi(0)$ . In this method it became difficult (or impossible) to find the appropriate  $\psi(0)$  and find a solution for large  $cn$  ( $> 20$ ). For large nonlinearity the secant method led to radially excited state for the appropriate  $\psi(0)$ . In the time-dependent method the only input is the value of  $cn$ . For a large  $cn$  in the repulsive case, the numerically obtained solution for the wave function shows many oscillations and is clearly unacceptable physically. A Crank-Nicholson-type approach was also used to solve the GP equation in three space dimensions [3]. The numerical instability also set a limit in that investigation in finding stationary ground-state solution for large values of nonlinearity.

For attractive interparticle interaction, the wave function is more sharply peaked at  $x = 0$  than in the case of the repulsive interparticle interaction and one has a smaller reduced number  $n$  and mean square radius  $\langle x^2 \rangle$ . In this case we find from Table I that with a reduction of the chemical potential  $\alpha$ , the reduced number  $n$  increases slowly and the mean square radius  $\langle x^2 \rangle$  decreases rapidly, so that the density of the condensate  $\rho \equiv n/\langle x^2 \rangle$  tends to diverge as  $n$  tends to a maximum value  $n_{\max}$ . The increase in density lowers the interaction energy. The kinetic energy of the system is responsible for the stabilization. As the central density increases further for stronger attractive interparticle interaction, kinetic energy can no longer maintain equilibrium of the system and the system collapses. Consequently, for  $n > n_{\max}$ , there is no stable solution of the GP equation. Numerically, from a plot of  $n$  versus  $1/\rho$  we find this maximum number consistent with  $\rho^{-1} = 0$  to be

$$n_{\max} \equiv \eta N_{\max} \approx 1.88. \quad (4.2)$$

There is no such limit on  $n$  in the repulsive case. In that case with the increase of the chemical potential  $\alpha$

the condensate increases in size as the number of particles in the condensate increases. These behaviors of the Bose-Einstein condensate in two dimensions were also noted in three dimensions [10,11]. However, in three dimensions the corresponding maximum value was  $n_{\max} \equiv 4N_{\max}|a|/a_{\text{ho}} \approx 2.30$  [10].

Both the time-dependent and time-independent approaches are equally applicable for spherically-symmetric radially excited states. For the first excited state, with one node in the wave function, we verified that the convergence was as good as in the ground-state case reported here. However, it is a routine study and we do not report the results here.

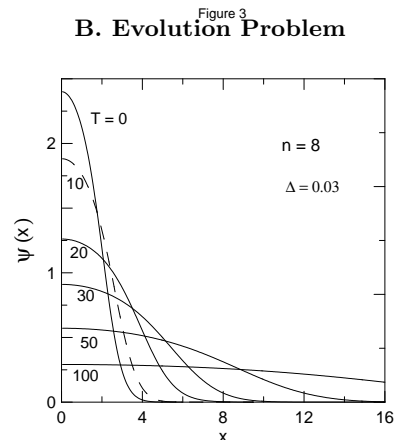


**Fig. 3.** Condensate wave function  $\psi(x)$  in the repulsive case at different times  $T = t/0.03$  for an expanding condensate after the trap is removed suddenly at  $T = 0$ . The initial condensate has  $n = 8$ , and the time evolution is performed using time step  $\Delta = 0.03$ ,  $\Delta_1 = 0.01$ , space step  $h = 0.0001$  and  $x_{\max} = 15$ .

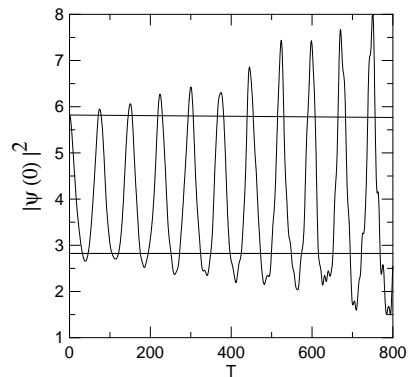


**Fig. 4.** The central probability density  $|\psi(0)|^2$  in the repulsive case at different times  $T = t/0.03$  for an oscillating condensate with  $n = 8$  after the trap energy is suddenly reduced to half at  $T = 0$ . The  $|\psi(0)|^2$  for condensates corresponding to the initial and final traps are denoted by the two straight lines. The time evolution is performed using time step  $\Delta = 0.03$ ,  $\Delta_1 = 0.01$ , space step  $h = 0.0001$ , and  $x_{\max} = 15$ .

Next we consider two time-evolution problems using the time-dependent method. We consider the ground state in the repulsive case with  $cn = 8$ . In the first problem, at  $t = 0$ , the trap is suddenly removed. In the second, at  $t = 0$ , the trap energy is suddenly reduced to half of the starting value. In both cases we study how the system evolves with time by solving the time-dependent GP equation using time step  $\Delta = 0.03$ ,  $\Delta_1 \sim 0.01$  and space step  $h = 0.0001$ . Both these problems are intrinsic time-dependent problems and can be studied numerically and experimentally.

The condensate cannot exist in the absence of the trap. In the first case after the trap is removed at  $t = 0$ , the radius of the condensate increases and the wave function extends over a larger region of space. We solve the time-dependent GP equation at different times. In Fig. 3 we plot the wave function at different reduced times  $T = t/0.03$ . The condensate increases in size monotonically with time and eventually disappears.

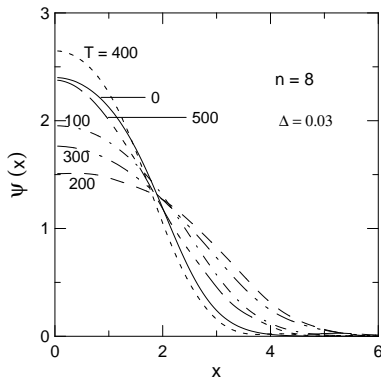


**Fig. 5.** Condensate wave function  $\psi(x)$  at different times  $T = t/0.03$  for an oscillating condensate after the trap energy is suddenly reduced to half at  $T = 0$ . All parameters are the same as in Fig. 3.

In the second problem at  $t = 0$ , we reduce the trap energy suddenly to half of the initial value corresponding to a stable final configuration for the condensate in the repulsive case. The system is now found to oscillate between the initial and final stationary states. In the absence of the nonlinearity, the system executes sinusoidal oscillations between the two stable configurations. However, in this nonlinear problem the system executes oscillations with evergrowing amplitude. To illustrate this oscillation we plot in Fig. 4 the the central probability density  $|\psi(0)|^2$  versus reduced time  $T = t/0.03$ . The  $|\psi(0)|^2$  for condensates corresponding to the initial and final trap energies are denoted by the two straight lines. We see that the oscillation increases with time. In our numerical study we find that after a very large number of iterations (several thousands) the amplitude may become very large. However, we do not know if this result makes sense physically as the cumulative numerical error of the type shown in Fig. 2 will also grow after a very large number of iterations, which will possibly invalidate our

conclusion. However, the solution presented in Fig. 4 is stable numerically and is the acceptable physical solution of the problem after a small number of iterations. This interesting behavior can possibly be observed experimentally and deserves further theoretical and numerical studies. In Fig. 5 we plot the wave functions of the system at different times which have very acceptable and smooth behavior. As the number of particles of the system continues fixed, the wave functions of smaller amplitudes have larger spacial extension [mean square radius (2.9)] so that the normalization condition (2.8) is preserved.

## V. SUMMARY

In this paper we present a numerical study of the Gross-Pitaevskii equation for BEC in two space dimensions under the action of a harmonic oscillator trap potential for bosonic atoms with attractive and repulsive interparticle interactions using time-dependent and time-independent approaches. Both approaches are used for the study of the stationary problem. In addition some evolution problems were studied by the time-dependent approach. We derive the boundary conditions (3.3) and (3.4) of the solution of the dimensionless GP equations (2.6) and (2.7). These boundary conditions are used for the solution of the stationary problem using both the time-dependent and time-independent approaches.

The time-dependent GP equation is solved by discretizing it using a Crank-Nicholson-type scheme, whereas the time-independent GP equation is solved by numerical integration using the four-point Runge-Kutta rule. In both cases numerical difficulty appears for large nonlinearity ( $cn > 20$ ). For medium nonlinearity, the accuracy of the time-independent method can be increased by reducing the space step  $h$ . However, the solution of the time-dependent approach exhibits intrinsic oscillation with time iteration which is independent of space and time steps used in discretization.

The ground-state wave function is found to be sharply peaked near the origin for attractive interatomic interaction. For a repulsive interatomic interaction the wave function extends over a larger region of space. In the case of an attractive potential, the mean square radius decreases with an increase of the number of particles in the condensate. Consequently, a stable solution of the GP equation can be obtained for a maximum number of particles in the condensate as given in Eq. (4.2).

In addition to the stationary problem we studied two evolution problems using the time-dependent approach. A stable bound state is considered and the trap potential is suddenly removed or reduced to half at  $t = 0$ . If the trap is removed suddenly, the system gradually and monotonically increases in size with time and eventually it disappears occupying the whole space with zero density. If the trap energy is suddenly reduced to half, the system oscillates around the two stationary positions.



The amplitude of the oscillation continue to increase with time. This behavior is interesting and can be studied experimentally in the future.

The work is supported in part by the Conselho Nacional de Desenvolvimento Científico e Tecnológico Fundação de Amparo à Pesquisa do Estado de São Paulo of Brazil.

- 
- [1] M. H. Anderson, J. R. Ensher, M. R. Mathews, C. E. Wieman, and E. A. Cornell, *Science* **269**, 198 (1995); J. R. Ensher, D. S. Jin, M. R. Mathews, C. E. Wieman, and E. A. Cornell, *Phys. Rev. Lett.* **77**, 4984 (1996); K. B. Dadić, M. O. Mewes, M. R. Andrews, N. J. van Druten, D. S. Durfee, D. M. Kurn, and W. Ketterle, *Phys. Rev. Lett.* **75**, 3969 (1995); D. G. Fried, T. C. Killian, L. Willmann, D. Landhuis, S. C. Moss, D. Kleppner, T. J. Greytak, *Phys. Rev. Lett.* **81**, 3811 (1998).
- [2] M. Edwards and K. Burnett, *Phys. Rev. A* **51**, 1382 (1995).
- [3] P. A. Ruprecht, M. J. Holland, K. Burnett, and M. Edwards, *Phys. Rev. A* **51**, 4704 (1995).
- [4] F. Dalfovo and S. Stringari, *Phys. Rev. A* **53**, 2477 (1996), S. Giorgini, L. P. Pitaevskii, and S. Stringari, *Phys. Rev. A* **54**, R4633 (1996); M. Edwards, P. A. Ruprecht, K. Burnett, R. J. Dodd, and C. W. Clark, *Phys. Rev. Lett.* **77**, 1671 (1996).
- [5] M. J. Holland, D. S. Jin, M. L. Chiofalo, and J. Cooper, *Phys. Rev. Lett.* **78**, 3801 (1997).
- [6] A. Gammal, T. Frederico, and L. Tomio, *Phys. Rev. E* **60**, 2421 (1999).
- [7] M. L. Chiofalo, S. Succi and M. P. Tosi, *Phys. Lett. A* **260**, 86 (1999); M. M. Cerimele, M. L. Chiofalo, F. Pistella, S. Succi, and M. P. Tosi, *Phys. Rev. E* **62**, xxx (2000); *Comput. Phys. Comm.*, in press.
- [8] E. A. Hinds, M. G. Boshier, and I. G. Hughes, *Phys. Rev. Lett.* **80**, 645 (1998); M. Bayindir and B. Tanatar, *Phys. Rev. A* **58**, 3134 (1998).
- [9] W. J. Mullin, *J. Low Temp. Phys.* **106**, 615 (1997); **110**, 167 (1998).
- [10] F. Dalfovo, S. Giorgini, L. P. Pitaevskii, and S. Stringari, *Rev. Mod. Phys.* **71**, 463 (1999).
- [11] R. J. Dodd, M. Edwards, C. J. Williams, C. W. Clark, M. J. Holland, P. A. Ruprecht, and K. Burnett, *Phys. Rev. A* **54**, 661 (1996); C. C. Bradley, C. A. Sackett, and R. G. Hulet, *Phys. Rev. Lett.* **78**, 985 (1997).
- [12] E. P. Gross, *Nuovo Cimento* **20**, 454 (1961); L. P. Pitaevskii, *Zh. Eksp. Teor. Fiz.* **40**, 646 (1961)[*Sov. Phys. JETP* **13**, 451 (1961)].
- [13] P. C. Hohenberg, *Phys. Rev.* **158**, 383 (1967).
- [14] V. Bagnato and D. Kleppner, *Phys. Rev. A* **44**, 7439 (1991).
- [15] J. J. Rehr and N. D. Mermin, *Phys. Rev. B* **1**, 3160 (1970); R. Masut and W. J. Mullin, *Am. J. Phys.* **47**, 493 (1979); H. A. Gersch, *J. Chem. Phys.* **27**, 928 (1957).
- [16] D. Ceperley, M. H. Kalos, and J. L. Lebowitz, *Phys. Rev. Lett.* **41**, 313 (1978).
- [17] S. E. Koonin, *Computational Physics*, Benjamin/Cummings Pub. Co. Inc., Menlo Park, 1986, pp 29-31, 161-167.
- [18] W. V. Houston and G. C. Phillips, *Principles of Quantum Mechanics*, North Holland Pub. Co., Amsterdam, 1973, pp 70 - 73.
- [19] R. Dautray and J.-L. Lions, *Mathematical Analysis and Numerical Methods for Science and Technology*, vol. 6 *Evolution Problems II*, Springer Verlag, Berlin, 1993, pp 45-47.
- [20] H. W. Wyld, *Mathematical Method for Physics*, W. A. Benjamin, Inc., Reading, 1976, pp 61-63